Absolute Photoionization Cross Sections of Excited He States in the Near-Threshold Region

Gisselbrecht, M; Descamps, D; Lyngå, C; L'Huillier, Anne; Wahlström, Claes-Göran; Meyer, M

Published in:
Physical Review Letters - Moving Physics Forward

DOI:
10.1103/PhysRevLett.82.4607

1999

Absolute Photoionization Cross Sections of Excited He States in the Near-Threshold Region

M. Gisselbrecht,[1,2] D. Descamps,[3] C. Lyngå,[3] A. L'Huillier,[3] C.-G. Wahlström,[3] and M. Meyer[1,2]
[1]*L.U.R.E., Centre Universitaire Paris-Sud, Bâtiment 209D, F-91898 Orsay Cedex, France*
[2]*CEA/DRECAM/SPAM, CEN Saclay, F-91105 Gif-sur-Yvette, France*
[3]*Department of Physics, Lund Institute of Technology, Box 118, S-22100 Lund, Sweden*
(Received 4 January 1999)

The absolute photoionization cross sections of the excited, short-lived He^* $1s2p\ ^1P$ and $1s3p\ ^1P$ states are determined experimentally in the region close to the He^+ $1s\ ^2S$ threshold (from 0 to 2 eV). The intermediate He^* states are prepared by photoabsorption of a high-order harmonic of an intense picosecond tunable laser and subsequently ionized by absorption of photons of several fixed frequencies, ranging from the near infrared to the ultraviolet. Our experimental results quantitatively confirm earlier theoretical work. [S0031-9007(99)09309-6]

PACS numbers: 32.70.Fw, 32.80.Fb, 42.65.Ky

The simple two-electron helium atom represents one of the showcase systems for the study of photon-atom interaction, and, in particular, of photoionization processes (for a review, see Ref. [1]). The direct ionization of ground state He has been studied extensively and the photoionization cross section is very well understood theoretically and experimentally [2]. Other recent examples underlining its model character deal with interference effects in two-electron excitations [3], circular dichroism in the double photoionization [4,5], new Rydberg series and resonances in doubly excited He [6], or photoionization and Compton double ionization up to photon energies of 20 keV [7].

Much less is known about photoionization of *excited* He atoms. Apart from early attempts on metastable He^* $(2s\ ^1S)$ and $(2s\ ^3S)$ [8], as well as on the short-lived $np\ ^1P$ and $np\ ^3P$ states ($n = 3$–5) [9,10], the knowledge of the photoionization of excited He states, especially of the energy-dependent cross section, has progressed only by theoretical efforts (e.g., [11,12], and references therein). This lack of experimental data is caused mainly by the high excitation energies (>20 eV) necessary to optically pump the excited states of helium, which are difficult to reach with conventional laser systems. Although techniques using synchronized synchrotron light and laser pulses are promising [13], the number of excited He atoms obtained remains too low to perform the kind of measurements presented in this manuscript.

The remarkable advance in the development of high-power short-pulse laser systems during the past decade has led to a new extreme-ultraviolet (XUV) photon source based on the generation of high-order harmonics of an intense laser pulse in a rare gas jet [14]. High-order harmonic generation provides coherent, linearly polarized XUV light in short pulses of high brightness, which opens new experimental possibilities, especially related to studies of time-dependent processes. Recently, high harmonics of a picosecond laser system have been used to measure the (subnanosecond) lifetimes of excited states in helium and carbon monoxide [15,16].

In this Letter, we report on the first experimental determination of the energy dependence of the photoionization cross sections for the He^* $1s2p\ ^1P$ and He^* $1s3p\ ^1P$ excited states, in the region close to the He^+ $1s\ ^2S$ ionization threshold. The short-lived ^1P states are populated by absorption of high-order (13th or 14th) harmonics of an intense picosecond tunable laser system and subsequently ionized by a probe laser with variable pulse energy and frequency. The photoionization cross section of the excited He^* $1s2p\ ^1P$ state is measured to be 16.6 Mb (1 Mb $= 10^{-18}$ cm^2) close to threshold and 6.6 Mb at about 1.3 eV above it, in good agreement with theoretical calculations [12,17]. This strong decrease of the cross section in the near-threshold region is even more pronounced for the photoionization of the He^* $1s3p\ ^1P$ state. At threshold, the cross section $\sigma(3p)$ is about 1.5 times higher than $\sigma(2p)$, but becomes of similar value at higher photon energy. This energy-dependent behavior reflects the spatial extension of the excited p-orbitals and emphasizes thereby one basic aspect of cross-section measurements.

The two-photon pump-probe excitation scheme is depicted in Fig. 1. In a first step, ground state He atoms are resonantly excited to the He^* $1s2p\ ^1P_1$ or the He^* $1s3p\ ^1P_1$ states. In a second step, the outer electron is promoted to the He^+ $1s\ ^2S$ continuum by a probe laser pulse. By varying the frequency of the probe laser, electrons of different kinetic energies are produced and different regions of the photoionization continuum are investigated. Since in the present study only one continuum (He^+ $1s\ ^2S$) can be reached with the photon energies used, the detection of He^+ ions is completely equivalent to electron detection, and the measured number of He^+ ions reflects directly the photoionization cross section in the investigated near-threshold region.

Part of the experimental setup has already been described elsewhere [15] and only a brief description will be given here. As shown in Fig. 2, the setup includes two different optical pathways starting from the same

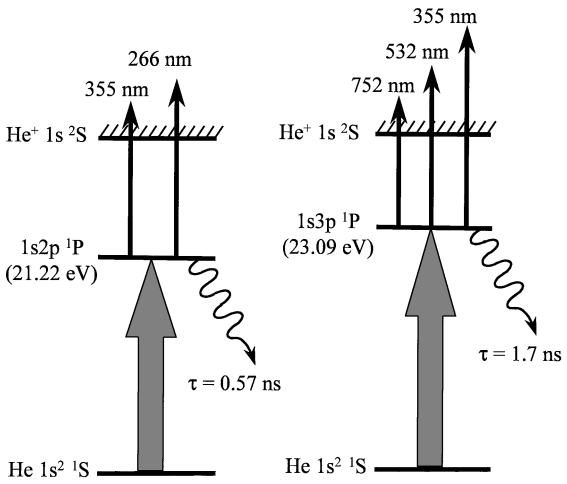

FIG. 1. Energy diagram of atomic helium showing schematically the two-photon excitation pathways used for the photoionization of the He^* $1s2p$ ^1P and He^* $1s3p$ ^1P excited states.

primary 1064-nm-wavelength Nd-YAG laser, operating at a 10 Hz repetition rate. One beam is frequency doubled and used to pump a distributed feedback dye laser oscillator which provides a tunable source of 70 ps pulses in the near-infrared range. These pulses are then amplified up to a mean energy of about 30 mJ. Finally, they are focused into a krypton gas jet to generate the high-order harmonic radiation. A spherical grating selects one harmonic order and focuses this radiation in the center of the experimental chamber. A slit placed before the experimental chamber allows us to eliminate the other harmonic orders and the fundamental beam. In order to excite the He^* $1s2p$ ^1P resonance at 21.22 eV (58.4 nm), the 13th harmonic of the dye laser tuned at the wavelength 760 nm is selected. For the He^* $1s3p$ ^1P resonance at 23.09 eV (53.7 nm), the dye laser is tuned at the wavelength 752 nm and the radiation is frequency doubled before being sent into the Kr jet. The 7th harmonic of the frequency-doubled light (i.e., the 14th harmonic of the fundamental) is selected. The temporal width of the harmonics is measured to be about 30 ps [14] and the bandwidth, measured by detecting the number of ions (for a given probe energy and frequency) as a function of the dye laser wavelength around the $1s2p$ or $1s3p$ resonance, is 0.005 nm ($\Delta E_{\rm ph} = 2$ meV, $\Delta E_{\rm ph}/E_{\rm ph} = 10^{-4}$). The relatively narrow bandwidth of the harmonics ensures an efficient population of the resonant states, since the width of the transition is limited by Doppler broadening (about 0.15 meV). The number of harmonic photons per pulse in the interaction chamber is estimated to be 10^7.

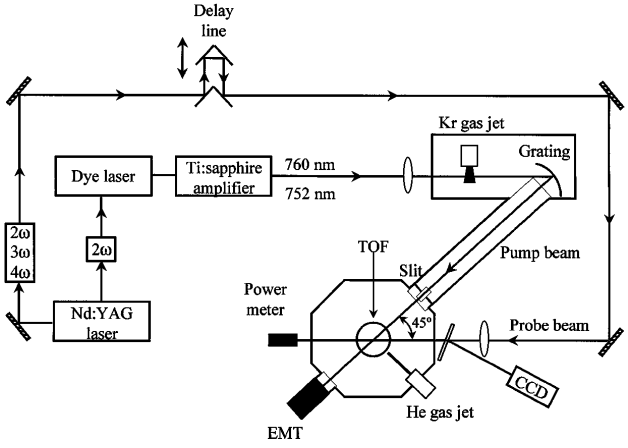

FIG. 2. Experimental setup for the measurement of photoionization cross sections from excited states in helium.

The other Nd-YAG beam is used to generate visible and UV photons for the ionization step, at wavelengths 532 nm (2nd harmonic), 355 nm (3rd), and 266 nm (4th) by frequency upconversion in KDP crystals. The probe laser energy can be varied between several μJ up to 1 mJ which corresponds to about 10^{12} to 10^{15} photons per pulse in about 70 ps duration. In addition, to ionize the He^* $1s3p$ excited state close to the threshold, the fundamental of the dye laser can be split into two beams, one used to generate the pump harmonic beam and the other used as a probe. This additional probe beam is not shown in Fig. 2.

The two light beams intersect at an angle of 45° in the center of the experimental chamber. They are linearly polarized, with the same polarization, set to be vertical (perpendicular to the plane of Fig. 2). The relative delay between the pump and probe pulses can be controlled and varied by an optical delay line. During the measurements, it is set to $\Delta\tau = 250$ ps in order to separate excitation and ionization steps. Both pump and probe pulses used in the experiment are sufficiently short so that the spontaneous decay of the excited states [$\tau(2p) = 0.57$ ns and $\tau(3p) = 1.7$ ns], during the excitation and ionization process, can be neglected. He gas of high purity is introduced into the experimental chamber by a synchronized pulsed gas nozzle. The produced ions are collected from the source volume by a high extraction field and mass analyzed in a conventional field-free time-of-flight spectrometer (placed perpendicular to the plane of Fig. 2). The energies of the probe and pump pulses are monitored for each laser shot using a photodiode and an electron multiplier, respectively.

Our determination of the absolute photoionization cross section is based on the saturation of the ionization step [18] (see below) and requires the measurement of the probe energy as well as the characterization of the spatial profiles of both pump and probe beams in the interaction region. The determination of the probe energy is done by calibrating the photodiode in absolute value using a power meter and by accounting for the transmission of the quartz window at the exit of the chamber. The uncertainty in the energy determination is estimated to $\pm 15\%$, mostly owing to a nonuniform transmission of the quartz window, and can be easily improved in future measurements. To characterize the probe spatial profile,

a beam splitter is placed before the vacuum chamber (see Fig. 2) and a small fraction of the probe beam is used to reproduce its spatial profile at the center of the chamber on a CCD camera. To determine the spatial profile of the pump beam, we measure the number of ions produced (for a given probe) as a function of the vertical position of the lens used to focus the probe beam. The curve obtained is proportional to the convolution of the probe and the pump spatial profiles. Typical values for the beam radii are about 100 μm and 500 μm for the probe and pump beam, respectively.

A typical experimental result obtained for He^* $1s2p$ with a probe wavelength of 355 nm is presented in Fig. 3. The number of ions is reported as a function of the probe energy. Each data point represents the integration over about 12 000 laser shots. The ion signal varies first linearly with the probe energy (see dashed line), and then saturates, because the ionization probability in the interaction region is close to one. Because of the relatively low number of photons in the pump beam, the excitation step in the present experiment is always far from saturation. The number of ions produced is equal to $N_{He^+} = \int \rho_{He^+}\, dV$, where the ion density ρ_{He^+} reads as

$$\rho_{He^+} = \rho_{He}\sigma_{exc}R_{pump}e^{-\Delta\tau/\tau}(1 - e^{-\sigma_{ion}R_{probe}}), \quad (1)$$

where ρ_{He} represents the neutral atom density, σ_{exc} (σ_{ion}) the excitation (ionization) cross section, $\Delta\tau$ the time delay between pump and probe pulses, τ the lifetime of the intermediate state, and R_{pump} (R_{probe}) the number of photons per cm^2 for the pump (probe) beam. For a given, constant pump energy, the saturation of the ion signal depends only on the product $\sigma_{ion}R_{probe}$. In ideal experimental conditions, where the probe beam would be much larger than the pump beam, so that R_{probe} could be considered as constant in the interaction region, the cross section σ_{ion} could simply be determined by fitting a curve $(1 - e^{-xR_{probe}})$ (x being the unknown parameter) to the experimental data. However, in our conditions, both beams vary in space over the interaction region. Therefore, we have to perform a three-dimensional integration in space of $R_{pump}(1 - e^{-xR_{probe}})$. In this expression, R_{probe} must be known exactly, but only the variation in space of R_{pump} is needed. Knowing the spatial profiles of both pump and probe beams, as well as the energy in the probe beam, this procedure allows us to determine the photoionization cross section in absolute value. Note that the number of ions continues to increase as a function of the probe energy, even far into the saturation regime (see Fig. 3). This is because the spatial region where ions can be produced and collected by the time-of-flight spectrometer increases.

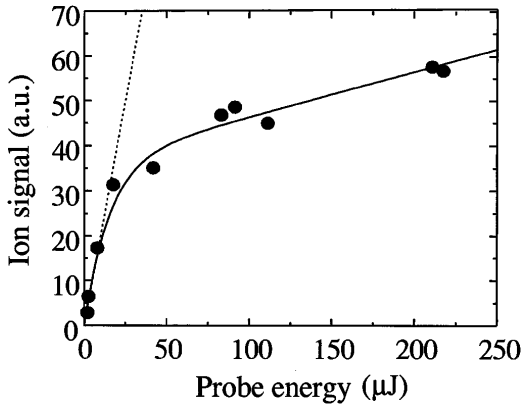

FIG. 3. Recorded number of He^+ ions as a function of the energy of the probe laser. The He atoms are prepared in the He^* $1s2p$ ^1P excited state, and the probe laser is set to a wavelength of $\lambda_P = 355$ nm. The dashed line indicates the linear, unsaturated regime. The solid line represents a fit to the experimental data using a three-dimensional integration as discussed in the text.

The experimental results for the determination of the absolute photoionization cross section of the excited He^* $1snp$ ^1P ($n = 2, 3$) states are summarized in Table I. In addition to the 15% uncertainty in the probe energy determination, we estimate the uncertainty due to the spatial profile measurements to be about 10%. The statistical error on the fits is typically of the order 15%–20%, resulting in a total uncertainty of about 25% for the determination of the cross section.

Theoretical calculations of photoionization cross sections usually present the total, *isotropic*, cross section σ_{ion}^{ISO}, obtained for an isotropic target ionized by unpolarized light (such that transitions between the magnetic sublevels $\Delta m = 0, \pm 1$ are allowed). Figure 4 shows theoretical results obtained using a B-spline-based configuration interaction calculation [12] (solid line) and those obtained by using a multiconfiguration Hartree–Fock method [17] (dashed line). Both calculations are practically superposed, which indicates that calculations of photoionization cross sections of excited states in helium have reached a high degree of accuracy. In our experiment, however, both light pulses are linearly polarized and the polarization vectors are chosen to be parallel. Only transitions between the magnetic sublevels $\Delta m = 0$ are allowed under these conditions. The He^* $1snp$ ^1P excited states can be ionized towards two

TABLE I. Experimentally determined absolute photoionization cross sections σ_{ion} for the He^* $1s2p$ ^1P and He^* $1s3p$ ^1P excited states as a function of the excess photon energy, defined as the difference between the probe photon energy and the ionization energy of the excited state. The total uncertainty for σ_{ion} is estimated to about 25%.

	λ_{probe} (nm)	E_{exc} (eV)	σ_{ion} (Mb)
He^* $1s2p$ $^1P_1$	355	0.12	16.6
	266	1.29	6.6
He^* $1s3p$ $^1P_1$	752	0.15	24.4
	532	0.83	10.5
	355	1.99	4.2

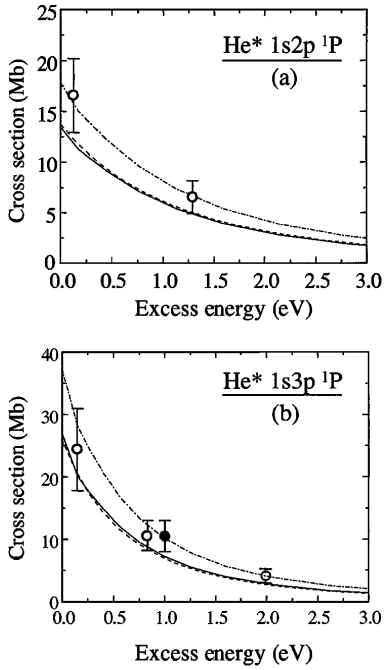

FIG. 4. Photoionization cross section of He* $1s2p\ ^1P$ (a) and He* $1s3p\ ^1P$ (b) as a function of the excess energy E_{exc}. The symbols ("∘": present work; "•": Ref. [9]) represent the experimental values, the lines (solid [12]; dashed [17]) are the theoretical isotropic cross sections, the dotted-dashed line is the theoretical cross section ([12]) modified to account for two-photon excitation with parallel (linear) polarization.

ionization continua corresponding to outgoing εs and εd waves. The cross section $\sigma_{\mathrm{ion}}^{\mathrm{PARA}}$ corresponding to our experimental conditions can be derived from the isotropic partial cross sections σ_s^{ISO} and σ_d^{ISO} by elementary angular algebra or by density matrix formalism [19] as $\sigma_{\mathrm{ion}}^{\mathrm{PARA}} = 3\sigma_s^{\mathrm{ISO}} + 6/5\sigma_d^{\mathrm{ISO}}$. (The isotropic cross section $\sigma_{\mathrm{ion}}^{\mathrm{ISO}}$ is equal to the sum $\sigma_s^{\mathrm{ISO}} + \sigma_d^{\mathrm{ISO}}$.) The theoretical cross sections for parallel polarizations, obtained by using the (isotropic) partial photoionization cross sections of Ref. [12] and applying the above formula, are shown as a dotted-dashed line in Fig. 4. This curve can be compared directly to our experimental results (open symbols), as well as to the experimental measurement of Dunning and Stebbings at $E_{\mathrm{exc}} = 0.95$ eV, (solid symbol) using similar polarization conditions to ours [9]. The agreement is excellent. Our experimental data confirm clearly the theoretical predictions of a stronger energy dependence for $\sigma_{\mathrm{ion}}(3p)$ than for $\sigma_{\mathrm{ion}}(2p)$ in the investigated near-threshold region. This tendency is predicted to continue for higher He* $1snp$ $(n > 3)$ excited states [12] and reflects the increasing spatial delocalization of the excited electron.

In conclusion, we have determined experimentally the absolute photoionization cross sections from the He* $1s2p\ ^1P$ and He* $1s3p\ ^1P$ excited states in the near-threshold region. The use of synchronized short laser pulses in a pump-probe arrangement allows us to overcome the experimental problems related to measurements on short-lived intermediate states. This method can easily be extended to other atomic or molecular systems, and can be improved to yield more precise measurements. Finally, we can vary the relative polarization of the two beams, which should enable the determination of partial photoionization cross sections.

We would like to thank Z. Felfli and S. Manson for providing us with their unpublished data for the photoionization cross sections, and A. N. Grum-Grzhimailo for his help in discussing the polarization effects. M. G. and M. M. would also like to thank the Lund Laser Center for support and hospitality. This work was supported by the European Community via the TMR-grant "Access to Large Scale Facilities," Contract No. ERBFMGECT950020(DG12). We acknowledge support from the Swedish Natural Science Research Council.

[1] V. Schmidt, Rep. Prog. Phys. **55**, 1483 (1992).
[2] J. A. R. Samson *et al.*, J. Phys. B **27**, 887 (1994).
[3] A. Menzel *et al.*, Phys. Rev. Lett. **75**, 1479 (1995).
[4] J. Viefhaus *et al.*, Phys. Rev. Lett. **77**, 3975 (1996).
[5] V. Mergel *et al.*, Phys. Rev. Lett. **80**, 5301 (1998).
[6] K. Schulz *et al.*, Phys. Rev. Lett. **77**, 3086 (1996).
[7] J. C. Levin *et al.*, Phys. Rev. Lett. **76**, 1220 (1996).
[8] R. F. Stebbings *et al.*, Phys. Rev. Lett. **30**, 815 (1973).
[9] F. B. Dunning and R. F. Stebbings, Phys. Rev. Lett. **32**, 1286 (1974).
[10] M. Ya. Amusia *et al.*, Sov. Phys. JETP **49**, 439 (1979).
[11] T. N. Chang and M. Zhen, Phys. Rev. A **47**, 4849 (1993).
[12] T. N. Chang and T. K. Fang, Phys. Rev. A **52**, 2052 (1995); **52**, 2638 (1995).
[13] J. Lacoursière *et al.*, Nucl. Instrum. Methods Phys. Res., Sect. A **351**, 545 (1994).
[14] A. L'Huillier *et al.*, J. Nonlinear Opt. Phys. Mater. **4**, 647 (1995).
[15] J. Larsson *et al.*, J. Phys. B **28**, L53 (1995).
[16] P. Cacciani *et al.*, Astrophys. J. **499**, L223 (1998).
[17] Z. Felfli and S. Manson (private communication).
[18] V. N. Ischenko *et al.*, J. Sov. Laser Res. **2**, 120 (1981).
[19] S. Baier *et al.*, J. Phys. B **27**, 3363 (1994).